Microstructure control to reduce leakage current of medium and high voltage ceramic varistors based on doped ZnO

Antoine Izoulet, Sophie Guillemet-Fritsch, Claude Estournès, Jonathan Morel

Microstructure control to reduce leakage current of medium and high voltage ceramic varistors based on doped ZnO

Antoine Izoulet [a,b,*], Sophie Guillemet-Fritsch [a], Claude Estournès [a], Jonathan Morel [b]

[a] *Université Toulouse, UMR CNRS-UPS-INP 5085, 118 Route de Narbonne, 31062 Toulouse Cedex 9, France*
[b] *TRIDELTA Parafoudres S.A., Boulevard de l'Adour, 65200 Bagnères de Bigorre, France*

Abstract

The leakage current (I_f) and the non-linearity coefficient (α) are crucial parameters in varistors. This work, deals with the optimization of the electrical characteristics of medium and high voltage varistors based on the $ZnO–Bi_2O_3–Sb_2O_3$ system. First, the aim was to allow the formation and the stabilization of the spinel phase by reducing the heating rate. To do so, the right sintering temperature and dwell time have to be chosen to obtain a breakdown field suitable for industrial requirements. During cooling, the spinel phase can return to a pyrochlore phase, which contributes to the increase of leakage current. In a second part, this reaction was prevented by faster cooling in an appropriate temperature range. The fine-tuning of both the heating and cooling phases leads to a significant decrease of the leakage current. Moreover, the value of the non-linearity coefficient was increased by 80%, due to better and more homogeneous wetting of the ZnO grains by the Bi-rich phase.

Keywords: Leakage current; Microstructure; Pyrochlore; Varistor; Zinc oxide

1. Introduction

Mainly developed from zinc oxide (ZnO), MOVs (Metal Oxide Varistors) present a strong nonlinear current–voltage characteristic.[1,2] Varistors are characterized by the threshold (or breakdown) voltage U_s ($=U_{1mA}$), at which point they switch from a very high conductive state to a strongly insulating state, and the coefficient of non-linearity α. In normal operation (i.e. below its threshold voltage), or when returning to normal conditions following a surge operation, the varistor lets a small current through, the leakage current I_f. The leakage current must be as low as possible.

It is well known that the electrical properties of MOVs are directly related to the microstructure and to the formulation of the material.[3] U_s is mainly governed by ZnO grain size. With the composition used in this work, i.e. $ZnO–Sb_2O_3–Bi_2O_3$ (ZSB), the microstructure consists of a majority of ZnO grains in a continuous and interconnected network of bismuth-rich phases. These Bi-rich phases are located at the grain boundaries and at the triple junctions of ZnO grains. The Bi-rich network also includes a phase with a spinel structure $Zn_7Sb_2O_{12}$ mainly localized at triple junctions of ZnO grains.[4–7] Olsson et al. showed that this configuration is necessary to obtain the desired varistor effect and to allow efficient oxygen transport during post-sintering annealing. But this continuous Bi-rich skeleton around ZnO grains can also provide an additional current contributing to an increased leakage current.[8] Stucki and Greuter[9] correlated the increase of I_f to the presence of an excess of oxygen in these areas. The present work focused on the Bi-rich phases to try to minimize their amount in the ceramic. However, due to the multiplicity of different polymorphic phases of Bi_2O_3,[10,11] and their proportions, which varies strongly with the sintering conditions and the formulation, it is difficult to control their formation and the amount produced. Moreover due to the high volume of medium (LDC1) and high (LDC2) voltage varistors (50 and 72 cm^3 respectively), a large thermal gradient occurs

* Corresponding author at: Institut Carnot CIRIMAT, UMR 5085 CNRS-UPS-INP, 118 route de Narbonne, 31062 Toulouse Cedex 09, France.
Tel.: +33561557475/6283.
E-mail addresses: antoine.izoulet@tridelta.fr, antoine.izoulet@gmail.com (A. Izoulet), guillem@chimie.ups-tlse.fr (S. Guillemet-Fritsch), estournes@chimie.ups-tlse.fr (C. Estournès), jonathan.morel@tridelta.fr (J. Morel).

http://dx.doi.org/10.1016/j.jeurceramsoc.2014.05.033

between the core and the surface, complicating the control of the distribution of such secondary phases. Nevertheless in the ZSB system, other Bi-rich phases appear. The pyrochlore phase (PY) $Bi_3Zn_2Sb_3O_{14}$, is formed after reaction between Sb_2O_3, ZnO and Bi_2O_3, in the early stages of sintering. This phase decomposes from 850 °C to yield the spinel phase (SP).[6] However, this last reaction is reversible upon cooling. It has been described[10,12] that the PY phase has both ionic and electronic conductivities which tend to increase the leakage current. Olsson et al.[13] argue that the PY phase has a detrimental effect on the efficiency of the ZnO/ZnO interface to act as an electrical barrier. The PY structure is essential to microstructure development because it avoids ZnO grain growth, it retains the Bi_2O_3, thereby avoiding its premature volatilization. Moreover, it might reduce grain boundary mobility.[2,14] But the PY phase is undesirable after sintering. Greuter et al.[15] showed that the absence of this phase does not affect the nonlinear properties of the varistor since it is not directly involved in the nonlinear behavior. The reactions of formation, decomposition and reformation of the PY phase are described below[6,16]:

$$3Sb_2O_4 + 4ZnO + 3Bi_2O_3 + 3O_2 \rightarrow 2Bi_3Zn_2Sb_3O_{14} \quad (> 500^\circ C)$$

$$2Bi_3Zn_2Sb_3O_4 + 17ZnO \rightarrow 9Zn_{2,33}Sb_{0,67}O_{14} + 3Bi_2O_3 \quad (> 850\,^\circ C)$$

$$3Zn_{2,33}Sb_{0,67}O_4 \rightarrow Zn_7Sb_2O_{12} \quad (> 950\,^\circ C)$$

$$3Zn_7Sb_2O_{12} + 3Bi_2O_3 \rightarrow 2Bi_3Zn_2Sb_3O_{14} + 17ZnO \quad (\text{slowcooling})$$

Several possibilities can be explored to prevent the formation or the reformation of the $Bi_3Zn_2Sb_3O_4$ phase. First it is possible to change the composition and especially the ratio of Sb_2O_3 to Bi_2O_3. It has been shown that a formulation with a Sb/Bi ratio $\gg 1$ enables the formation of PY phase during sintering.[16] Another way to control the formation of the PY is to act on the cooling rate. Rapid cooling (quenching) from high temperature would result in the absence of PY phase. However, no varistor behavior is observed for samples quenched from these temperatures. PY phase is responsible for the varistor effect due to the presence of potential barriers.[4,14] Peiteado et al.[17] decided to reduce the proportion of PY in the final ceramic by stabilizing the spinel phase and preventing the reformation of $Bi_3Zn_2Sb_3O_{14}$ upon cooling. The structure of the spinel phase allows the incorporation of various cations in its empty octahedral and tetrahedral sites. This phase will therefore be able to dissolve cations from other additives. It has been reported that cations such as Co, Ni or Mn were incorporated in order to improve the properties of the varistor and its stability.[18,19] Peiteado obtained optimized varistors by adding both TiO_2 and SiO_2, the titanium cations thus can enter in the spinel lattice and stabilize this phase, and SiO_2 reacts with ZnO to form the insulating Zn_2SiO_4 phase.

Given the large number of additives necessary to obtain optimized nonlinear properties, the incorporation of further substances may modify these characteristics. Indeed, interactions between components are not excluded. Our aim is to limit drift of the electrical characteristics. Finally changing the Sb/Bi ratio will result in a modification of the threshold voltage. Indeed we want to obtain a breakdown field between 180 and 200 V mm^{-1} at 1 mA DC.

In this study, it was decided to work on another way to control the microstructure, i.e. the sintering cycle, trying to adapt the cycle to minimize the presence of PY phase in the varistor. Firstly, we defined a new sintering cycle which gives the right good decomposition of PY phase and better stabilization of the SP phase. In order to succeed, the heating rate up to the sintering temperature was studied. The sintering temperature and the dwell time were explored to obtain the best non-linear properties and an appropriate breakdown field. To complete this first step, we focused on how to limit SP phase decomposition during cooling by studying the influence of cooling rate in a selected range of temperatures.

2. Experimental procedure

2.1. Sample preparation

The samples, based on the ZSB system, were produced following the conventional way of preparing ceramics. The raw materials were industrial grade chemicals. The formulation of the samples includes: ZnO, Sb_2O_3 (Ms), Bi_2O_3 (Mb), Co_3O_4, Mn_2O_3, NiO, B_2O_3, $Al(NO_3)_3{\cdot}9H_2O$, with Ms/Mb = 2.30. The oxide mixture was ground energetically in distilled water for 5 h. Binders were added and the solution spray dried. The green ceramics were pressed at 100 MPa (LDC1) or at 95 MPa (LDC2) in cylindrical pellets 58 mm in height and 48.5 mm (LDC1) or 57.8 mm (LDC2) in diameter. A first heat treatment (400 °C – 10 °C h^{-1}) was performed to remove the binders.

In the present study, the influence of several parameters on the final properties of the varistors LDC1 was evaluated using a Taguchi method.[20] In order to limit the number of tests we focused on three factors, presenting no interactions between them, at three levels. The testing of all combinations between each level theoretically requires 3^3 (27) tests. To reduce this number, a full two-factor map was constructed (Table 1-a), including 9 tests, which was added to a Latin square 3×3 (Table 1-b). The final plan is shown in Table 1-c.

These selected parameters were the sintering temperature, the heating rate from 950 °C to the final temperature, and the sintering time. The temperature is controlled by rings (Ferro). The shrinkage dependence on temperature of these rings is known and listed in abacus. The description of all sintering tests on LDC1 varistors are shown in Table 2.

In the first part of this paper, electrical tests on LDC1 varistors were carried out in order to assess the effects of the parameters altered during the sintering study. Then, tests on varistors with higher energy capabilities (LDC2) were conducted (Table 2).

Table 1
Work methodology (F = factor).

A		
F1		F2
1		1
1		2
1		3
2		1
2		2
2		3
3		1
3		2
3		3
B		
1	2	3
2	3	1
3	1	2
C		
F1	F2	F3
1	1	1
1	2	2
1	3	3
2	1	2
2	2	3
2	3	1
3	1	3
3	2	1
3	3	2

One varistor was sintered at 1095 °C for 2.5 h **(MOVA)**, another at 1115 °C for 5 h **(MOVB)** and a last one at 1115 °C for 5 h with accelerated cooling **(MOVC)**. Usual tests consist of measuring tension at low current (from 1 mA to 10 A) and at high current (from 500 A to 100 kA).

2.2. Characterization

Prior to the electrical characterization, the varistors were embedded within a dielectric glass layer. Then two opposite surfaces of the coated varistor were polished and an aluminum electrode deposited by sputtering on each side. The sintered varistors were 40 mm in diameter (LDC1) and 48 mm for superior energy capability (LDC2) and the height was 40 mm for both. The current–voltage of the varistors was measured at low current (pre-breakdown and breakdown zone) using a DC generator Spellman Electronics. For the determination of the $U(I)$ curve at high currents, a current impulse 8/20 μs generator was used. The residual voltage at 10 kA was determined using a Yokogawa 120 oscilloscope via a 10-fold voltage divider.

The current leakage I_f was determined at room temperature under a voltage of $0.5 \times U_{1mA}$ (DC).

The coefficient of nonlinearity α given by (1) was determined from 1 mA to 10 mA using the following relation:

$$\alpha = \frac{log(I_1/I_2)}{\log(U_1/U_2)} \quad (1)$$

The clamping voltage R given by Eq. (2) allows the evaluation of the extent of the nonlinear zone and the performance of varistor. It should as low as possible.

$$R = \frac{U_{10\,kA}(V)}{U_{1\,mA}(V)} \quad (2)$$

Electrical tests were carried out according to ICE 60099-4 standard.

The microstructure of samples and the nature of the phases were examined using a scanning electron microscope (SEM – JEOL JSM-6400) coupled to an energy dispersive X-ray spectrometry (EDX) system from Oxford Instruments.

3. Results and discussion

• LDC1 varistors

Fig. 1 shows the influence of the sintering parameters on breakdown field (E_s) at I = 1 mA. Each point corresponds to the average value of tests performed on 5 different samples.

An increase in heating rate led to an increase of the breakdown field while the opposite effect was noted for the dwell time. The influence of the sintering temperature is not straightforward.

Table 2
Sintering conditions for the study of LDC1 (ϕ = 40 mm, h = 40 mm) and LDC2 (ϕ = 48 mm, h = 40 mm) varistors.

Type of varistor	Sample	Sintering parameters		
		Heating rate (°C h^{-1})	Sintering temperature (°C)	Sintering time (h)
LDC1 (Φ40 mm)	1	10	1105	0
	2	10	1105	0.5
	3	10	1105	1
	4	15	1110	0.5
	5	15	1110	1
	6	15	1110	0
	7	20	1115	1
	8	20	1115	0
	9	20	1115	0.5
LDC2 (Φ48 mm)	MOV A	20	1095	2.5
	MOV B	20	1115	5
	MOV C	20	1115	5[a]

[a] Fast cooling.

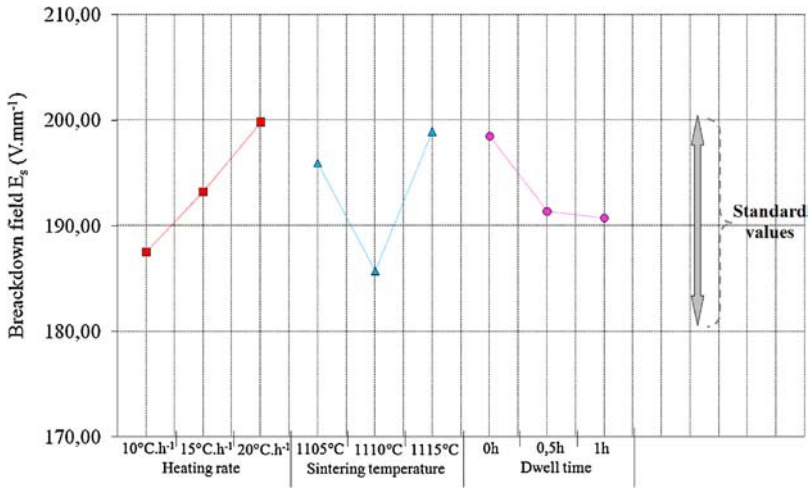

Fig. 1. Graph of average effect: influence of the sintering parameters on the breakdown field E_s (at 1 mA DC).

It is well known that the switching voltage is related to the ZnO grain size. The higher the sintering temperature and/or the longer the dwell time, the larger the ZnO grain size is. With large ZnO grains, the threshold voltage (or threshold field) should be low. Nevertheless we note that the increase of the sintering temperature does not lead to the desired effect. The minimum was reached at 1110 °C, and at 1115 °C the threshold field value was higher (Fig. 1).

The coefficient of non-linearity α is only slightly influenced by the heating rate and the dwell time (Fig. 2). As noted for the breakdown field, the variation of α with the sintering temperature was not monotonous. Nevertheless, the temperature of 1115 °C seemed to have a beneficial effect on non-linearity compared to the other temperatures. The variation of α usually follows the variation of the threshold voltage: α was inversely proportional to the threshold voltage.

Fig. 3 shows the effect of the sintering parameters on the leakage current measured $0.5 \times U_{1\,\mathrm{mA}}$ (V). The sintering temperature had a major effect on I_f, the minimum value 0.36 µA was obtained at 1115 °C. The value of I_f was also very sensitive to the other parameters. The value of I_f was minimal for a slow heating rate (10 °C h^{-1}) and a sintering time of 1 h.

Among the different sintering parameters, the sintering temperature has a major effect on the electrical characteristics of varistors. The threshold voltage is very sensitive to the changes in each sintering cycle. A fast heating rate leads to a smaller grain size and therefore a significant increase of the threshold voltage. We determined the optimum dwell time at 1 h. The grain size, and thus, the voltage are mainly dependent on the sintering temperature. Nevertheless obtaining a higher threshold field shows that the grain size of ZnO is not the only parameter governing E_s.

- LDC2 varistors

The optimized sintering parameters were adapted for varistors of higher energy capacity, i.e. a larger diameter (48 mm). Because of industrial specifications, the value of the threshold field E_s has to be between 170 and 190 V mm^{-1}. Due the higher volume, the heating rates and the sintering times have to be optimized and are different from those of the previous experimental plan. The results obtained were compared with data obtained

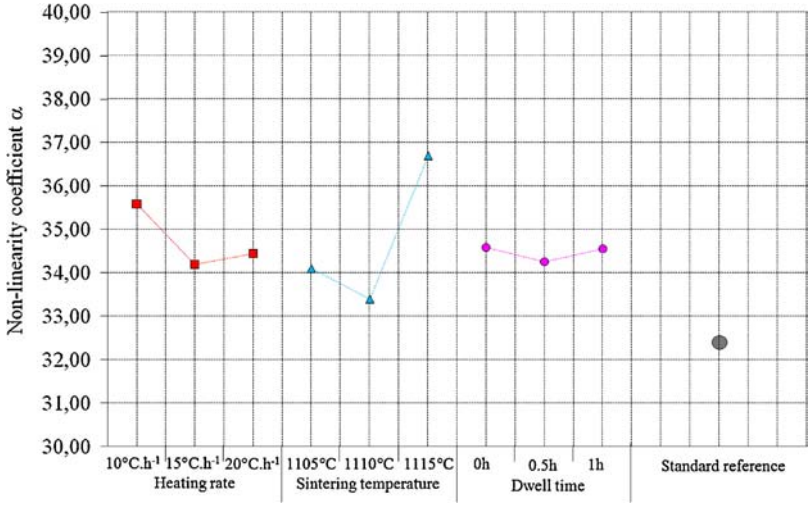

Fig. 2. Graph of average effect: influence of the sintering parameters on the nonlinearity coefficient α (calculated between 10^{-3} and 10^{-2} A cm^{-2}).

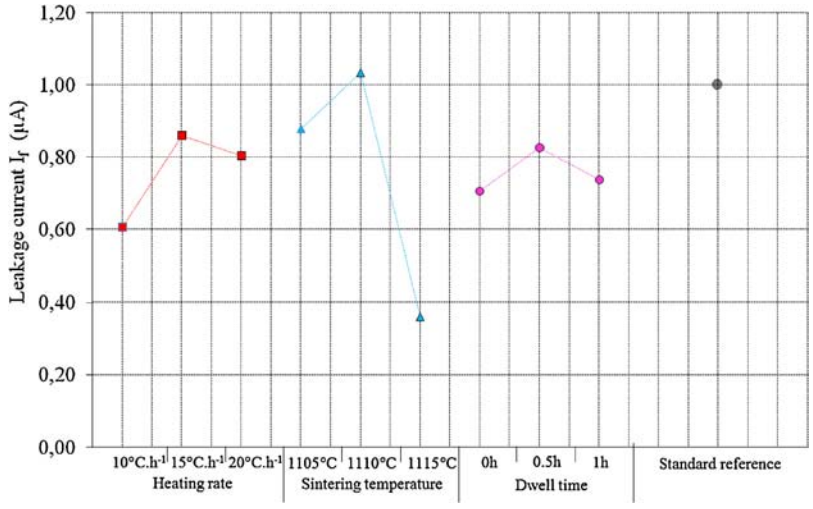

Fig. 3. Graph of average effect: influence of the sintering parameters on the leakage current I_f at $0.5 \times U_{1\,mA}$ (V) DC.

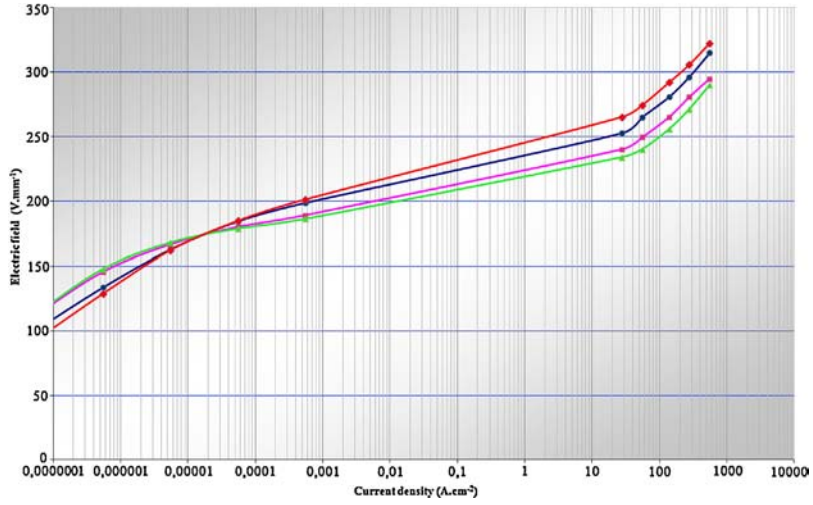

Fig. 4. *I–U* characteristics of different varistors (♦: Standard, ●: MOV A, ■ MOV B, ▲: MOV C).

from a standard commercial varistor. The details are given in Table 3.

Concerning samples A and B, increases of both the sintering time and temperature had a positive effect on the leakage current, the coefficient of non-linearity and the ratio (Table 3) but the sintering time had a negligible effect on E_s. Indeed, a slight decrease in E_s was observed. The cooling at 150 °C h^{-1} performed on MOV C seems to improve the varistors' electrical properties.

These changes in the sintering cycle led to a reduction by more than 80% of the value of the leakage current and at the same time increase the coefficient α by 111%. There was no major change in the value of the threshold field. Finally, the decrease of R was mainly due to a strong decrease in the residual tension $U_{res10\,kA}$ (−1290 V).

The current–voltage characteristics of the four varistors are plotted in Fig. 4.

In order to check the influence of the sintering parameters on the microstructure, SEM observations were performed on a standard varistor and on varistor C (Figs. 5 and 6). The two ceramics clearly show different microstructures. Both present the characteristic elements of a varistor microstructure: ZnO

Table 3
Electrical measurements of LDC2 samples T_f: sintering temperature – $E_s = U_{1mA}/h$ – $U_{res10\,kA}$: residual tension at 10 kA – I_f: leakage current at $0.75 \times U_{1\,mA}$ – α: non-linearity coefficient calculated between $J = 10^{-3}$ and 10^{-2} A cm^{-2} – R: clamping voltage $R = U_{res10\,kA}/U_{1\,mA}$.

Sample ID	Sintering conditions (heating rate – T_f – dwell time)	E_s (V mm^{-1})	$U_{res10\,kA}$ (V)	I_f (µA)	α	R
Stand.	70 °C h^{-1} – 1095 °C – 2.5 h	185	12,900	17	27	1.745
MOV A	20 °C h^{-1} – 1095 °C – 2.5 h	185	12,500	13.2	31	1689
MOV B	20 °C h^{-1} – 1115 °C – 5 h	180	11,800	4.7	47	1638
MOV C	20 °C h^{-1} – 1115 °C – 5 h – fast cooling	179	11,610	3.4	56	1626

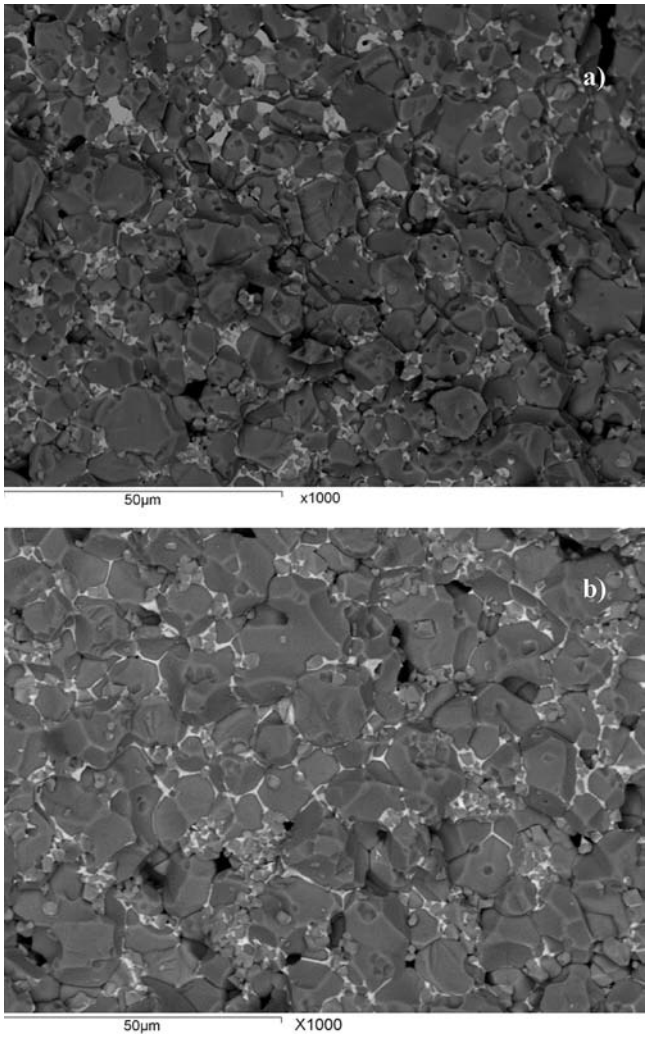

Fig. 5. SEM images of standard MOV (a) and of MOV C (b) (×1000). ZnO grains appear in dark gray, spinel phase in light gray and the bright white regions are Bi-rich phases.

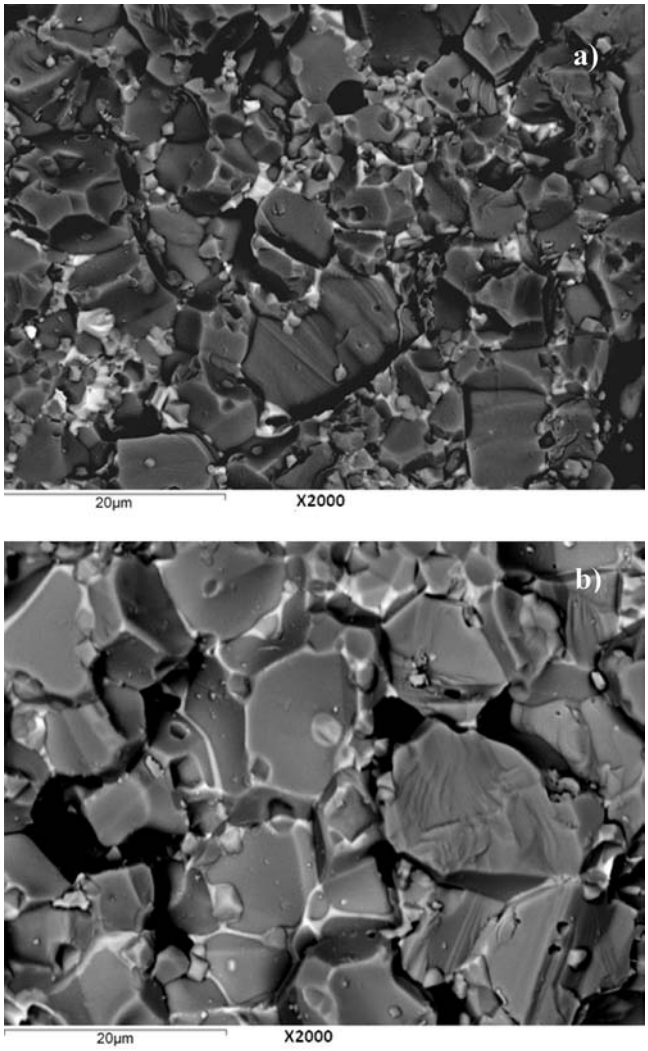

Fig. 6. SEM images of standard MOV (a) and of MOV C (b) (×2000). ZnO grains appear in dark gray, spinel phase in light gray and the bright white regions are Bi-rich phases.

grains appear in dark gray, spinel phase in light gray and the bright elements are Bi-rich phases. The size of the ZnO grains ranges from 10 to 15 µm for each sample. Nevertheless, a lot of bright phases, in the form of clusters, are observed at the triple junctions. The MOV C shows many Bi-rich intergranular phases at the homo- and triple junctions (Fig. 6). Moreover ZnO grain wetting seems to be improved in varistor C. SEM observations on polished samples (Fig. 7) confirm the difference in microstructure between standard varistor A and sample C. Unlike the standard varistor, which exhibited some Bi-rich clusters, the MOV C contained only Bi-rich phases located at the grain boundaries. X-ray cartography (Figs. 8 and 9) confirmed the absence of the PY phase. It also showed that Sb and Bi were not located in the same phase.

4. Discussion

The heating rate and sintering temperature appeared to be the most crucial parameters to control in order to improve the electrical properties of the ceramics. The decrease of the heating rate, before the sintering temperature, provides both a high non-linear coefficient α and a low leakage current. However there is also a slight decrease in the threshold field.

The threshold field decrease accompanying the decrease of heating rate is due to an increase of the grain size and therefore a smaller number of grain boundaries. The decrease of the heating rate also allows more time for PY decomposition into the spinel phase. This PY decrease thus explains the decrease in leakage current as observed by Metz and Clayton.[10,12] The value of threshold field observed at 1115 °C which was higher than the one observed at 1110 °C could be explained by a change in the grain boundary voltage. Olsson and Dunlop[21] demonstrated that according to the nature of the interfaces, the breakdown voltage can vary by a few volts from one grain boundary to another one. The sharp decrease of leakage current at 1115 °C could be explained by a higher ratio of Bi_2O_3 evaporation.

The transposition of the optimized conditions to higher energy capability varistors confirms the trend that the electrical properties can be significantly improved when optimizing the

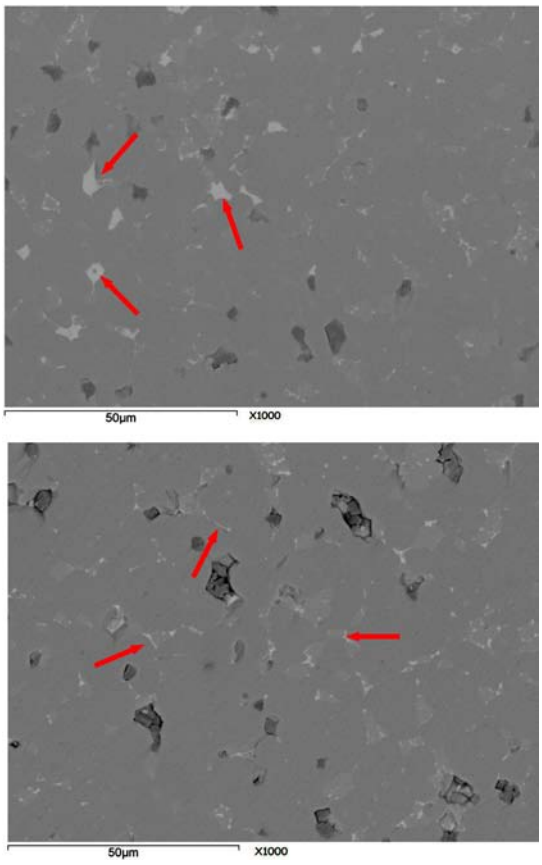

Fig. 7. SEM images of polished standard MOV (a) and of polished MOV C (b). ZnO grains appear in dark gray, spinel phase in light gray and the bright elements are Bi-rich phases. Arrows indicate the differences in morphology of Bi-rich phases between standard MOV (clusters) and MOV C (thin layers).

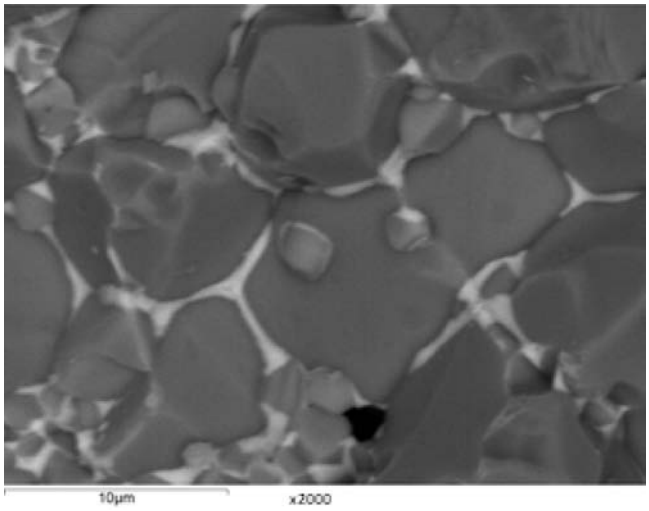

Fig. 8. SEM image of MOV C (×2000) (ZnO grains: dark gray, spinel phases: light gray, Bi-rich phases: bright).

sintering parameters. Without modifying E_s, the R parameter is strongly reduced. It is well known that it is the conductivity of ZnO grains that controls the high current region behavior.[2,22] The low current region, which is governed by the grain boundaries, seems to be more resistive. This is confirmed by the decrease of I_f. So, the sintering modifications seem to improve the non-linearity at high currents and the high resistivity at low currents. SEM observations agree with this pattern. MOVC, which is sintered with an optimized cycle, presents a homogeneous microstructure, devoid of PY. The higher cooling rate, associated with a slow heating rate, prevented the reappearance of PY. This faster cooling also avoids dewetting of

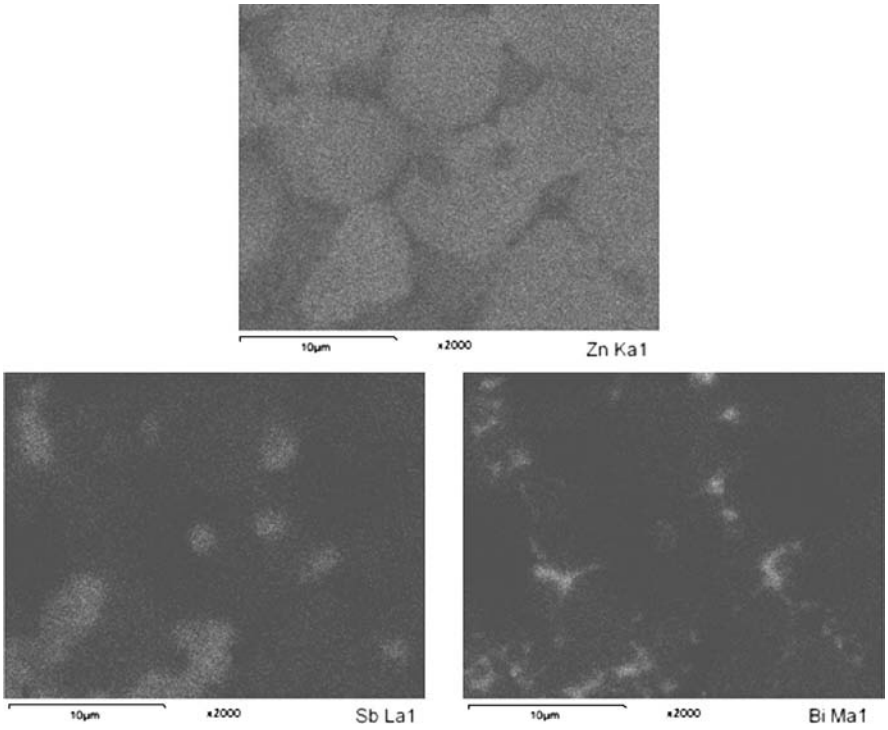

Fig. 9. X-ray mapping of MOV C.

ZnO grains by Bi_2O_3. Indeed, compared to a standard varistor, which had a majority of clusters of Bi_2O_3-rich phases at the triple junctions, MOV C exhibited an interconnected network composed of the Bi-rich phase that totally wets all the ZnO grains. This homogeneity and the continuity of the coating between ZnO grains provide better non-linear properties.

5. Conclusion

The improvement of electrical performance, including the reduction of leakage current, by the control of microstructure in ZnO based varistors was investigated. The sintering cycle was optimized to reduce the final amount of pyrochlore phase (in medium and high voltage varistors). The reduction of the heating rate associated with appropriate sintering temperature and dwell time lead to a decrease of the leakage current and an increase of the non-linearity coefficient α. The new parameters we suggest allow a better spinel phase formation from the pyrochlore phase and its stabilization. An accelerated cooling rate in a selected range of temperatures avoids the reverse reaction SP to PY. This new sintering cycle provides varistors with high non-linearity and a strongly reduced leakage current. The microstructure of the optimized varistors showed no pyrochlore phase and a better ZnO grain wetting by the intergranular Bi-rich phase. These results show that the varistor behavior at low and high current can be improved without changing the formulation. It will be interesting to study the varistor behavior and the leakage current behavior at high temperature. Adding some minor dopants, to modify the resistivity of grain boundaries and the conductivity of ZnO grains, could lead to highly nonlinear varistors showing high degradation resistance.

References

1. Matsuoka M. Non-ohmic properties of zinc oxide ceramics. *Jpn J Appl Phys* 1971;**10**:736–46.
2. Gupta TK. Applications of zinc oxide varistors. *J Am Ceram Soc* 1990;**73**:1817–40.
3. Clarke DR. Varistor ceramics. *J Am Ceram Soc* 1999;**82**:485–502.
4. Wong J. Microstructure and phase transformation in a highly non-ohmic metal oxide varistor ceramic. *J Appl Phys* 1975;**46**:1653–9.
5. Santhanam AT, Gupta TK, Carlson WG. Microstructural evolution of multicomponent ZnO ceramics. *J Appl Phys* 1979;**50**:852–9.
6. Inada M. Microstructure of nonohmic zinc oxide ceramics. *Jpn J Appl Phys* 1978;**17**:673–7.
7. Clarke DR. The microstructural location of intergranular metal-oxide phase in a zinc oxide varistor. *J Appl Phys* 1978;**49**:2407–11.
8. Olsson E, Dunlop G. Development of interfacial microstructure during cooling of a ZnO varistor material. *J Appl Phys* 1989;**66**:5072–7.
9. Stucki F, Greuter F. Key role of oxygen at zinc oxide varistor grain boundaries. *Appl Phys Lett* 1990;**57**:446–8.
10. Metz R, Delalu H, Vignalou JR, Achard N, Elkhatib M. Electrical properties of varistors in relation to their true bismuth composition after sintering. *Mater Chem Phys* 2000;**63**:157–62.
11. Onreabroy W, Sirikulrat N, Brown AP, Hammond C, Milne SJ. Electrical properties of a ZnO–CoO–Bi_2O_3 varistor. *Solid States Ion* 2006;**177**:411–20.
12. Clayton J, Takamura H, Metz R, Tuller HL, Wuensch BJ. The electrical and defect properties of $Bi_3Zn_2Sb_3O_{14}$ pyrochlore: a grain-boundary phase in ZnO-based varistors. *J Electroceram* 2001;**7**:113–20.
13. Olsson E, Dunlop G, Osterlund R. Development of functional microstructure during sintering of a ZnO varistor material. *J Am Ceram Soc* 1993;**76**: 65–71.
14. Mergen A, Lee WE. Microstructural relations on BZS Pyrochlore-ZnO mixtures. *J Eur Ceram Soc* 1997;**17**:1049–60.
15. Greuter F, Hagemeister M, Beck O, Osterlund R, Kessler R. High Field Strengh Varistor Material. European Patent n° 2305622; 2011.
16. Peiteado M, De la Rubia MA, Fernandez JF, Caballero AC. Thermal evolution of ZnO–Bi_2O_3–Sb_2O_3 system in the region of interest for varistors. *J Mater Sci* 2011;**41**:2319–25.
17. Peiteado M, Reyes Y, Cruz AM, Calatayud DG, Fernandez-Hevia D, Caballero AC. Microstructure engineering to drastically reduce the leakage currents of high voltage ZnO varistor ceramics. *J Am Ceram Soc* 2012;**95**:3043–9.
18. Inada M. Formation mechanism of nonohmic zinc oxide ceramics. *Jpn J Appl Phys* 1980;**19**:409–19.
19. Kato T, Kawanata I, Yamada A, Ishibe S, Kobayashi M, Takada Y. Effect of Ni and Cr one the stability of leakage current for spinel-reduced ZnO varistor ceramics. *J Ceram Soc Jpn* 2011;**119**:234–7.
20. Taguchi G. Introduction to quality engineering. In: *Designing quality into products and processes.* White Plains, NY: Krause International Publication; 1986.
21. Olsson E, Dunlop GL. The effect of Bi_2O_3 content on the microstructure and electrical properties of ZnO varistor materials. *J Appl Phys* 1989;**66**:4317–24.
22. Houabes M, Bernik S, Talhi C, Bui A. The effect of aluminium oxide on the residual voltage of ZnO varistors. *Ceram Int* 2005;**31**:783–9.